Journal of Engineering and Applied Sciences 12 (Special Issue 3): 6492-6497, 2017
ISSN: 1816-949X

Modeling and Simulation of DC Offset in Wideband Direct Conversion Receivers

[1]Zi Hui Lau, [1]Heng Siong Lim and [2]Alan Wee Chiat Tan and [2]M.L. Sim
[1]Faculty of Engineering and Technology, Multimedia University, Cyberjaya, Selangor, Malaysia
[2]Penang Design Centre, Motorola Solutions Bayan Lepas, Penang, Malaysia

Abstract: The main challenge in multi-standard wideband receiver design is to achieve good sensitivity in the presence of strong out-of-band interference. In a typical development cycle of a new direct conversion receiver iterative process of receiver design and bench measurement iscarried out until satisfactory interference rejection performance is achieved. This time consuming design cycleis required due to the lack of realistic simulation models for various impairments such as the Direct Current (DC) offset at the baseband stage. To address this problem, anempirical model for DC offset of direct conversion receiver due to strong out-of-band interference is proposed. The proposed model allows DC offset of a direct conversion receiver to be simulated in order to facilitate convenient interference rejection design and analysis. The model has been fitted to both constant envelope Frequency Modulation (FM) interference and Time-Division Multiple-Access (TDMA) interference using measurement data. Experiments show that the model is capable of predicting DC offset for different interference powers and frequencies.

Key words: Direct conversion receiver, DC offset, modelling, interference, TDMA, experiments

INTRODUCTION

Direct Conversion Receiver (DCR) architecture is commonly adopted in the implementation of wireless communication devices due to its advantages in terms of cost, physical size and current consumption. However, DCRs often suffer from Direct Current (DC) offset issue which is caused by the presence of interference and hardware imperfections. For the conventional receiver, the out-of-band interference can be suppressed with a band-selection Surface Acoustic Wave (SAW) filter. Nevertheless, the off-chip SAW filter is expensive and bulky and has fixed center frequency and bandwidth. Driven by the trend towards wideb and reconfigurable receiver with lower cost, smaller form factor and lower power consumption the SAW-less wideb and receiver has gained popularity (Lin *et al*., 2015). Without the SAW filter, the receiver is exposed to both signal and interference present in the wideband range. Due to nonlinearity and other hardware imperfections, the presence of strong out-of-band interference induces a DC offset that may desensitize the receiver especially when the desired signal is weak. In the development of new RF receivers, time consuming and repetitive cycle of receiver circuit design and blocking performance measurement are normally carried out until satisfactory blocking performance is achieved. Normally, the blocking performance of a RF receiver is quantified by conducting bench measurement. However, due to the large number of test cases with different interferer types involved, the development cycle of a new product may take months solely for blocking optimization. This is not desirable from time to market point of view. To shorten the development cycle time it is desirable to have a behavioral DC offset model that allows Bit-Error-Rate (BER) simulation to be carried out for the evaluation of the impacts of different types of interference.

The reduction in sensitivity of a DCR due to DC offset can be attributed to the nonlinearity in the circuit and the RF interference self-mixing (Faulkner, 2002; Valkama *et al*., 2010; Choi and Choi, 2013). The latter is the result of finite isolation between the receiver Local Oscillator (LO) and RF input. The offset signal is a dynamic (or time-varying) signal due to varying squared envelope of the interference. In the literature, the dynamic DC offset is commonly modeled as a Gaussian process (Choi and Choi, 2013; Lindoff and Malm, 2002; Keshavarzi *et al*., 2011). However, the transient behavior for different types of interference remains less well understood. In the design of high performance wideband DCR, a better understanding of the transient behavior such as the autocorrelation property of the dynamic DC offset is required. In this study, we propose a simple model for describing the DC offset behavior that correlates to the RF envelop variation of the interference. Very good results are achieved when the model is fitted to measured data obtained from a SAW-less DCR.

MATERIALS AND METHODS

Interferer modeling: The presence of strong interference in a direct conversion receiver will result in non-linear

Corresponding Author: Zi Hui Lau, Faculty of Engineering and Technology, Multimedia University, Cyberjaya, Selangor, Malaysia

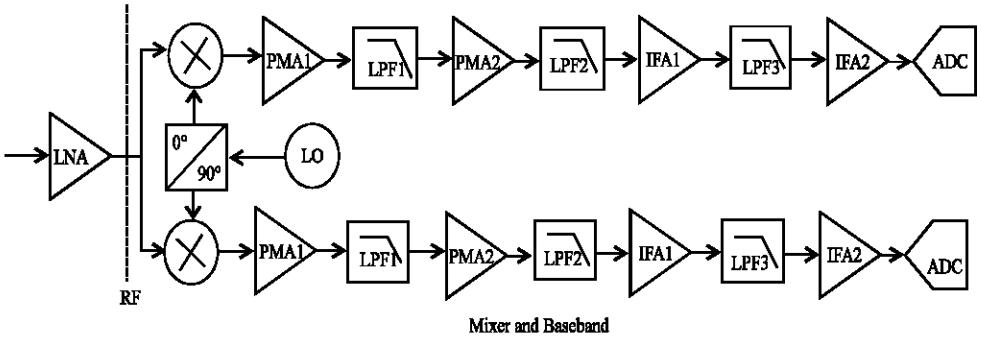

Fig. 1: Direct conversion receiver

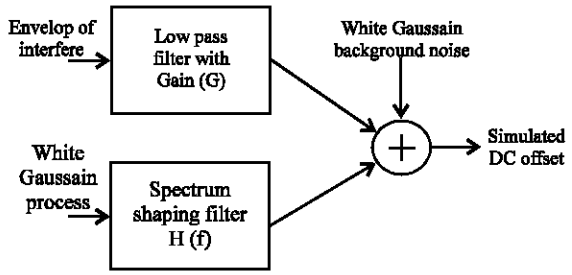

Fig. 2: DC offset random process modeling

distortion and subsequently manifest itself as DC offset at the baseband stage of the receiver. In the following study, the origin and impact of the DC offsets and two common types of interference found in the Land Mobile Radio system (Hess, 1993) are briefly described.

Direct conversion receiver: The block diagram of a typical direct conversion receiver (also known as the homodyne or zero-IF receiver) under study is as shown in Fig. 1.

The DCR converts the desired band directly to zero frequency and employs low-pass filtering to suppress interferers. It has several advantages over the heterodyne receiver such as elimination of the image rejection and bulky off-chip filtering requirements which makes it well suited for multiband and multi-standard operations. However, since the signal of interest is translated to baseband at the early stage of the receive chain without any filtering, strong out-of-band interference or blocking signals may induce a dynamic DC offset that will corrupt the signal and saturates the following stages. The DC offset is mainly due to the RF interference self-mixing and the even order nonlinearity of the receiver. For high performance DCR, the offset needs to be properly removed or compensated. A possible approach is to employ AC coupling at the mixer output. However, this approach is not suitable for signal with significant low frequency content as well as Time-Division Multiple Access (TDMA) system (Mashhour *et al*., 2001). Other approaches such as digital and hybrid analog-digital techniques have been used to remove the DC offset (Mailand and Jentsche, 2005). It is clear that in-depth understanding of the characteristics of the DC offset is required for the design and development of high performance DCR. However, very little has been done so far in characterizing the autocorrelation properties of the dynamic DC offset.

Interferers: In this study, we consider two types of out-of-band land mobile radio interferers namely a constant envelope FM and a TDMA 4-FSK signals. These are the two commonly used signal formats for commercial as well as public safety Land Mobile Radio services (Hess, 1993).

DC offset random process model: The block diagram of the DC offset random process model is shown in Fig. 2. There are three components that describe the overall DC offset variation over time. Firstly, the fast DC offset variation is modeled by a DC term with magnitude proportional to the instantaneous envelope/power of the interferer. Secondly, the slow varying DC offset variation is modeled as a correlated Gaussian process. The bandwidth of the slow variation is captured by the bandwidth of the spectrum shaping filter. Lastly, the background noise is modeled by the white Gaussian process.

The low pass filter is used for modeling the low pass characteristics of the overall receiver. The relationship between the average DC offset against the input interference power, the IIP2, IIP3 and gain of direct conversion receiver subsystems, may be represented by a Gain constant G.

In the following, we derive the relationship between the interference power and the DC offset power. The result is useful for determining the Gain G in the model. The output signal of the RF stage can be modeled using a simplified RF non-linearity model:

$$Y_{RF}(t) = \alpha_1 x_{RF}(t) + \alpha_2 x_{RF}^2(t) + \alpha_3 x_{RF}^3(t) \qquad (1)$$

Where:
α_1, α_2 and α_3 = The 1st, 2nd and 3rd order RF = Nonlinearity model coefficients, respectively

The received RF signal:

$$x_{RF}(t) = Re[\sqrt{2}x_1(t)e^{j\omega_1 t} + \sqrt{2}x_2(t)e^{j\omega_2 t}] \quad (2)$$

contains a desired signal around frequency and an interferer around frequency. Substituting Eq. 2 into 1 yields (Eq. 3) (refer to next page).

The mixer and BB non-linearities can be modeled using a memoryless polynomial model:

$$y'_{BB}(t) = \beta_1 y_{BB}(t) + \beta_2[y_{BB}(t)]^2 + \beta_3[y_{BB}(t)]^3 \quad (3)$$

where β_1, β_2 and β_3 are the BB nonlinearity model coefficients. It is assumed that the 3rd and higher-order nonlinearities are insignificant. $y_{BB}(t)$ is the result of down converting $y_{RF}(t)$ to baseband. The DC offset of baseband signal is mainly caused by the second-order nonlinearity of the mixer-BB stage. Consider only the second-order nonlinearity in Eq. 3, the DC offset can be obtained as Eq. 5:

$$\begin{aligned}
y_{RF}(t) = {} & Re\left\{\sqrt{2}\left[\alpha_1(x_1(t)) + \alpha_3\begin{pmatrix}\frac{3}{2}x_1(t)|x_1(t)|^2 + \\ 3x_1(t)|x_2(t)|^2\end{pmatrix}\right]e^{j\omega_1 t}\right\} + \\
& Re\left\{\sqrt{2}\left[\alpha_1(x_2(t)) + \alpha_3\begin{pmatrix}\frac{3}{2}x_2(t)|x_2(t)|^2 + \\ 3x_2(t)|x_1(t)|^2\end{pmatrix}\right]e^{j\omega_2 t}\right\} + \\
& Re\left\{\sqrt{2}\left[\frac{\sqrt{2}\alpha_2}{2}|x_1(t)|^2\right]e^{j(2\omega_1)t}\right\} + Re\left\{\sqrt{2}\left[\frac{\sqrt{2}\alpha_2}{2}|x_2(t)|^2\right]e^{j(2\omega_2)t}\right\} + \\
& Re\left\{\sqrt{2}\left[\sqrt{2}\alpha_2 x_1(t)x_2(t)\right]e^{j(\omega_1+\omega_2)t}\right\} + Re\left\{\sqrt{2}\left[\sqrt{2}\alpha_2 x_1(t)x_2^*(t)\right]e^{j(\omega_1-\omega_2)t}\right\} + \\
& Re\left\{\sqrt{2}\left[\frac{\alpha_3}{2}x_1^3(t)\right]e^{j(3\omega 1)t}\right\} + Re\left\{\sqrt{2}\left[\frac{\alpha_3}{2}x_2^2(t)\right]e^{j(3\omega 2)t}\right\} + \\
& Re\left\{\sqrt{2}\left[\frac{3\alpha_3}{2}x_1(t)|x_2(t)|^2\right]e^{j(\omega_1+2\omega_2)t}\right\} + Re\left\{\sqrt{2}\left[\frac{3\alpha_3}{2}x_1(t)|x_2^*(t)|^2\right]e^{j(\omega_1+2\omega_2)t}\right\} + \\
& Re\left\{\sqrt{2}\left[\frac{3\alpha_3}{2}x_2(t)|x_1(t)|^2\right]e^{j(\omega_1+2\omega_2)t}\right\} + Re\left\{\sqrt{2}\left[\frac{3\alpha_3}{2}|x_1(t)|^2x_2^*(t)\right]e^{j(2\omega_1-2\omega_2)t}\right\}
\end{aligned} \quad (4)$$

$$\begin{aligned}
DC = {} & \beta_2\left|\alpha_1 x_1(t) + \frac{3\alpha_3}{2}x_1(t)[x_1(t)]^2 + 3\alpha_1 x_1(t)[x_2(t)]^2\right|^2 + \\
& \beta_2\left|\alpha_1 x_2(t) + \frac{3\alpha_3}{2}x_2(t)[x_2(t)]^2 + 3\alpha_1[x_1(t)]^2 x_2(t)\right|^2 + \\
& \beta_2\left|\frac{\sqrt{2}\alpha_2}{2}[x_1(t)]^2\right|^2 + \beta_2\left|\frac{\sqrt{2}\alpha_2}{2}[x_2(t)]^2\right|^2 + \beta_2\left|\frac{\alpha_3}{2}[x_1(t)]^3\right|^2 + \\
& \beta_2\left|\frac{\alpha_3}{2}[x_2(t)]^3\right|^2 + \beta_2\left|\sqrt{2}\alpha_2 x_1(t)x_2(t)\right|^2 + \beta_2\left|\sqrt{2}\alpha_2 x_1(t)x_2^*(t)\right|^2 + \\
& \beta_2\left|\frac{3\alpha_3}{2}x_1(t)[x_2(t)]^2\right|^2 + \beta_2\left|\frac{3\alpha_3}{2}x_1(t)[x_2^*(t)]^2\right|^2 + \\
& \beta_2\left|\frac{3\alpha_3}{2}[x_1(t)]^2 x_2(t)\right|^2 + \beta_2\left|\frac{3\alpha_3}{2}[x_1(t)]^2 x_2^*(t)\right|^2
\end{aligned} \quad (5)$$

The values of the coefficients (α_1, α_2, α_3) and (β_1, β_2, β_3) can be determined based on the specifications of the RF and mixer-BB stages, respectively. For instance, the 1st-order coefficient α_1 is the small-signal voltage gain. The 2nd-order coefficient α_2 can be expressed in terms of the input-referred voltage intercept point for IM2:

$$\alpha_2 = -\frac{\alpha_1}{V_{11P2}} \quad (6)$$

Where $V_{IIP2} = \sqrt{2RL/1000}(10)^{IIP2/10}$ IIP2 is the 2nd-order input intercept point in dBm and RL is the load resistance (usually equal to 50 Ω). The 3rd-order coefficient α_3 can be expressed in terms of the input-referred voltage intercept point for IM3:

$$\alpha_3 = \frac{3}{4}\frac{\alpha_1}{V_{1P3}^2} \quad (7)$$

Where $V_{IIP2} = \sqrt{2RL/1000}(10)^{IIP3/10}$ IIP3 and is the 3rd-order input intercept point in dBm. The coefficients (β_1, β_2, β_3) can be determined in a similar way based on the specifications of the mixer-BB stage.

The slow offset variation behavior could be described by an autocorrelation function. From the measurement data analysis, a simple Gaussian function below is recommended:

$$R(\tau) = \frac{\sqrt{\pi}}{\gamma}e^{-\pi^2\tau^2\gamma^2} \quad (8)$$

where γ a parameter that controls the bandwidth of the Power Spectral Density (PSD) of the DC offset which is given by:

$$P(f) = e^{-\gamma^2 f^2} \quad (9)$$

This model is well suited for generating realizations of DC offsets for simulation study. To produce the DC offsets with the required correlation property the white Gaussian noise process can be used as the input to a linear spectrum shaping filter. The shaping filter can be designed as the square root of the magnitude of the PSD:

$$|H(f)| = |P(f)|^{1/2} \quad (10)$$

and the impulse response of the filter can be determined as:

$$h(t) = \frac{\sqrt{2\pi}}{\gamma} e^{-2\pi^2 t^2/\gamma^2} \quad (11)$$

which has a Gaussian shape. The proposed model simplifies the design and implementation of the spectral shaping filter and it also fits well with the measurement data as evident in this study.

RESULTS AND DISCUSSION

Model verification: Two different scenarios have been considered for DC offset measurement: out-of-band FM interference and out-of-band TDMA interference. The DCR used for the measurement is from a commercial device.

The received signals (at the output of the ADC) are measured with different interferer's center frequencies in the range 435-443 MHz (with increment of 1 MHz) and powers in the range -50 to +5 dBm (with increment of 5 dB). Since, the in-band frequency is assumed at 433 MHz, the interference is 2-10 MHz offset away from the desired signal. The sampling rate of the ADC is 40 kHz. The sensitivity of the receiver is around -120 dBm. Hence, the interference is about 70-125 dB stronger than the desired signal. To minimize the effect of the background noise, we have averaged the measured signal over three sets of data for every experiment.

Interference power versus DC offset power: Figure 3 shows the measured DC offset power versus interference power at frequency 438, 441 and 443 MHz. The result calculated using the model in Eq. 5 and the given specifications of the DCR used for measurement is also plotted in Fig. 3 for comparison.

It can be observed that the model is capable of characterizing the relationship between the DC offset power and the interference power.

Autocorrelation and power spectral density: The constant envelope FM interference is used for characterizing the slow time-varying behavior of the DC offset. The model defined in Eq. 8 and 9 are fitted to the measured data by estimating the parameter.

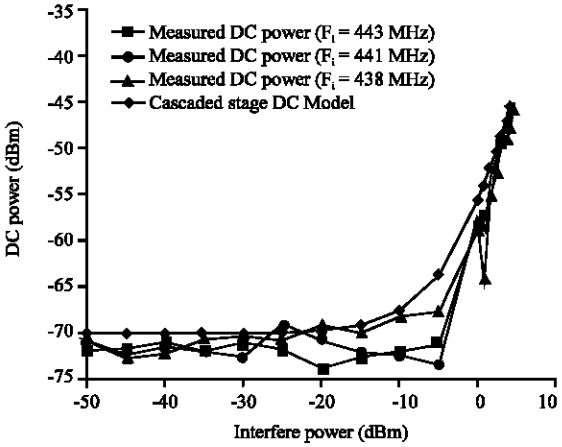

Fig. 3: DC offset power versus interference power

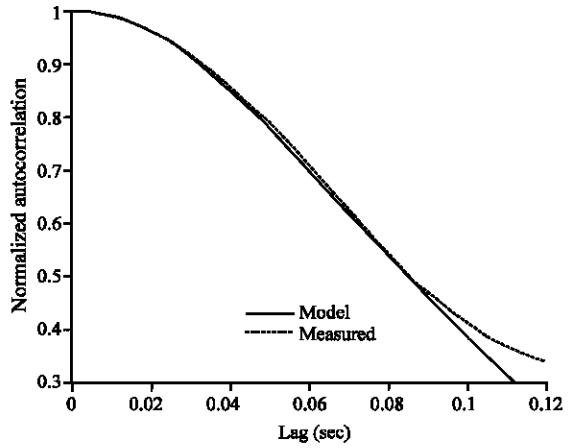

Fig. 4: Normalized autocorrelation of the DC offset due to FM interference at 435 MHz with +5 dBm power

Figure 4 shows a typical result of the model fit. The parameter is found to be 0.32. The value is applicable for all the tested interference frequencies and powers. From Fig. 5, the proposed model fits well with the estimated autocorrelation up to a lag of 0.09 sec. It can be also seen that the autocorrelation is quite high as the DC offset varies slowly in time. For the PSD, the proposed model works satisfactorily in modeling the slow-varying DC offset. The spectral contents above 12 Hz are due to background noise.

Figure 6 shows the measured and simulated DC offset due to an FM interference at 435 MHz with 5 dBm power. The solid line (at the center) of the Fig. 6 indicates the DC offset without background noise while the dotted line indicates the DC offset with background noise. Close examination of the Fig. 6 will reveal that the DC offset is slowly varying in time.

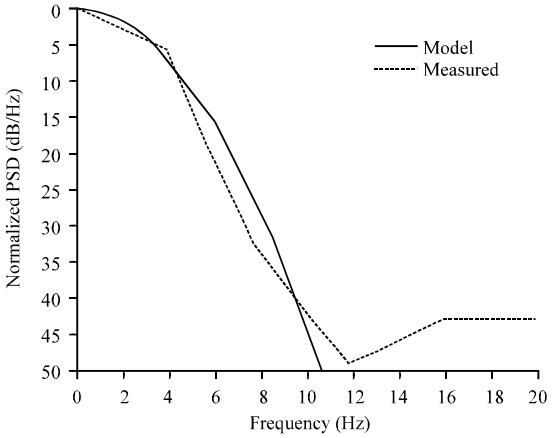

Fig. 5: Normalized power spectral density of the DC offset due to FM interference at 435 MHz with +5 dBm power

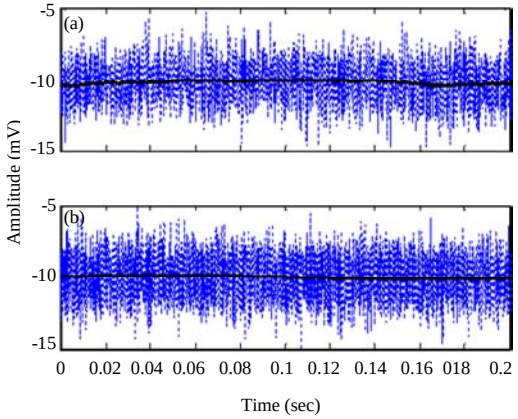

Fig. 6: Measured and simulated DC offset with background noise considering FM interference at 435 MHz with +5 dBm power (Dotted line = DC+noise, Solid line = DC): a) Measured DC offset and b) Simulated offset

Simulation of DC offset due to TDMA interference: The second measurement data for the TDMA interference are from the same range of frequencies and powers considered in the first experiment. The TDMA interference is a 4-FSK signal with a period of 60 sec (30 msec ON time). When the interference power is strong (i.e., above -20 dBm), the DC offset at the output of the receiver varies according to the ON/OFF nature of the TDMA interference (the upper plot of Fig. 7). We assume that the long term slow varying DC offset in this case has the same characteristics as the case of constant envelope (FM) interference discussed earlier. Therefore, the model developed above can be used for modeling the slow varying DC offset.

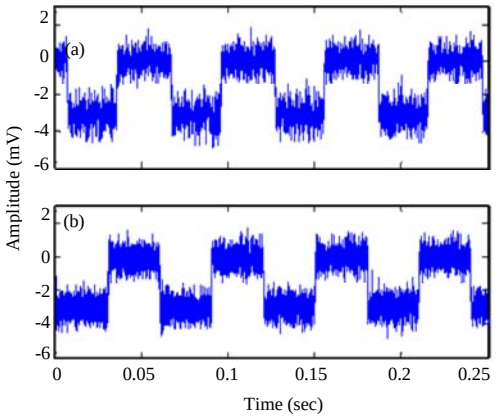

Fig. 7: Measured and simulated DC offset with background noise considering TDMA interference at 435 MHz with +3 dBm power; a) Measured DC offset and b) Simulated offset

For simulation, a rectangular wave is used for the envelope of the interference (Fig. 2). The gain of the low pass filter G can be determined according to the model in Eq. 5. Figure 7 (lower plot) shows the simulated DC offset due to TDMA interference at 435 MHz with 3 dBm power.

CONCLUSION

In this study, we have proposed an empirical model for the DC offset variation caused by strong out-of-band interference in a direct conversion receiver. This research is motivated by the lack of a behavioral DC offset model which is needed for the evaluation of the impacts of different types of interference via computer simulation. The model could capture both the long and short-term transient behaviors of the DC offsets for two interferer types, namely the constant envelope FM interferer and a TDMA signal with a given duty cycle. The simulated DC offset shows good agreement with measurement data for both the FM and TDMA interference scenarios. The current research is focused on utilizing the modelfor design and evaluation of out-of-band interference detection and mitigation schemes.

REFERENCES

Choi, M. and S. Choi, 2013. Performance analysis on the self-mixed interference cancellation in direct conversion receivers. IEEE. Trans. Consum. Electron., 59: 310-315.

Faulkner, M., 2002. DC offset and IM2 removal in direct conversion receivers. IEEE. Proc. Commun., 149: 179-184.

Hess, G.C., 1993. Land-Mobile Radio System Engineering. Artech House, Boston, Massachusetts, ISBN:9780890066805, Pages: 371.

Keshavarzi, M., A. Mohammadi, A. Abdipour and F.M. Ghannouchi, 2011. Characterization of DC offset on adaptive MIMO direct conversion transceivers. IEICE. Trans. Commun., 94: 253-261.

Lin, F., P.I. Mak and R.P. Martins, 2015. Wideband receivers: Design challenges, tradeoffs and state-of-the-art. IEEE. Circuits Syst. Mag., 15: 12-24.

Lindoff, B. and P. Malm, 2002. BER performance analysis of a direct conversion receiver. IEEE. Trans. Commun., 50: 856-865.

Mailand, M. and H.J. Jentschel, 2005. Compensation of dc-offsets and RF-self-mixing products in six-port-based analog direct receivers. Proceedings of the 14th International Conference on IST Mobile and Wireless Comm Summit, June 19-22, 2005, TU Dresden, Dresden, Germany, pp: 1-5.

Mashhour, A., W. Domino and N. Beamish, 2001. On the direct conversion receiver-a tutorial. Microwave J., 44: 114-128.

Valkama, M., A. Springer and G. Hueber, 2010. Digital signal processing for reducing the effects of RF imperfections in radio devices an overview. Proceedings of 2010 IEEE International Symposium on Circuits and Systems, May 30-June 2, 2010, IEEE, Paris, France, ISBN:978-1-4244-5308-5, pp: 813-816.